

Lawrence Berkeley National Laboratory

LBL Publications

Title

The Ethanol-Ethyl Acetate System as a Biogenic Hydrogen Carrier

Permalink

<https://escholarship.org/uc/item/4vb8z38r>

Journal

Energy Technology, 11(1)

ISSN

2194-4288

Authors

Mevawala, Chirag
Brooks, Kriston
Bowden, Mark E
et al.

Publication Date

2023

DOI

10.1002/ente.202200892

Copyright Information

This work is made available under the terms of a Creative Commons Attribution License, available at <https://creativecommons.org/licenses/by/4.0/>

Peer reviewed

The Ethanol–Ethyl Acetate System as a Biogenic Hydrogen Carrier

Chirag Mevawala, Kriston Brooks, Mark E. Bowden,* Hanna M. Breunig, Ba L. Tran, Oliver Y. Gutiérrez, Tom Autrey, and Karsten Müller*

Liquid organic hydrogen carriers will likely be a key element of a future hydrogen economy by enabling the storage and transport of large quantities of hydrogen. Ethanol is a liquid organic hydrogen carrier that is readily available from biological resources, which undergoes a reversible reaction to yield hydrogen and ethyl acetate. The objective of the present study is to obtain a better understanding of the thermodynamic and environmental suitability of the ethanol–ethyl acetate cycle for hydrogen storage applications. The analysis covers three aspects: thermodynamics of the chemical reaction, energy balance of the process, and a first-order assessment of greenhouse gas emissions. Thermodynamics of the reaction are characterized by a standard Gibbs energy of reaction close to zero which allows the reaction to be shifted between hydrogenation and dehydrogenation within a moderate window of temperature and pressure conditions. The energy demand for dehydrogenation is comparatively small, resulting in an overall system efficiency of 88%. A life cycle greenhouse gas analysis over a 20-year storage system lifetime gives a carbon intensity of 7.0 kg-CO_{2eq}/kg-H₂ delivered. These results indicate that the ethanol–ethyl acetate system has considerable promise as a hydrogen carrier and should be the subject of further research.

1. Introduction

The standard technology for hydrogen storage today is still compression. However, this technique only stores small amounts of energy per volume. To overcome low energy densities of elemental hydrogen storage technologies, carrier-based approaches for storage and transport have become the subject of intensive research.^[1] Organic liquids in particular have drawn much attention in this regard. Liquid organic hydrogen carriers (LOHCs) are mostly unsaturated compounds that take up hydrogen in a chemical reaction, forming the corresponding saturated species.^[2] The saturated species are generally cyclic hydrocarbons reducing the endothermicity to release H₂ to form the more stable aromatic substance.^[3] A huge advantage of this approach is the fact that hydrogen can be stored and transported safely under ambient pressure and temperature. Well-

known LOHC systems are toluene/methyl cyclohexane^[4] and oligomers of toluene like dibenzyl toluene/perhydro dibenzyl toluene (H0–/H18–DBT).^[5] These carriers provide a high storage density, but they suffer from requiring a high dehydrogenation temperature, reducing the overall system efficiency.

An alternative could be utilization of alcohols as carriers. Hydrogen release from alcohols is usually based on reforming.^[6] However, this leads to irreversible decomposition of the carrier. The purpose of this work is to evaluate ethanol as an LOHC system that can be dehydrogenated reversibly. This should be done under milder conditions than typical LOHCs through a reversible dehydrogenative coupling (DHC) reaction. This offers the potential of higher energy efficiency. In addition, ethanol is cheaper than most other LOHCs, and is not petroleum based, resulting in potentially lower greenhouse gas emissions.

DHC with alcohols is an interesting alternative to the hydrogenation of C=C double bonds.^[7] Alcohols offer several advantages as hydrogen carriers, including their availability, low cost, and low reaction temperatures.^[8] An example of a DHC reaction with an alcohol is the reaction of two ethanol molecules forming ethyl acetate and two hydrogen molecules^[9]




This reaction proceeds in two steps with the intermediate acetaldehyde

C. Mevawala, K. Brooks, M. E. Bowden, B. L. Tran, O. Y. Gutiérrez, T. Autrey
Pacific Northwest National Laboratory
Richland, WA 99352, USA
E-mail: Mark.Bowden@pnl.gov

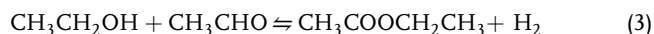
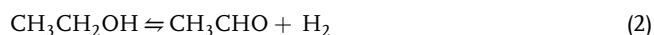
H. M. Breunig
Energy Analysis and Environmental Impacts Division
Lawrence Berkeley National Laboratory
Berkeley, CA 94720, USA

K. Müller
Institute of Technical Thermodynamics
University of Rostock
18059 Rostock, Germany
E-mail: karsten.mueller@uni-rostock.de

 The ORCID identification number(s) for the author(s) of this article can be found under <https://doi.org/10.1002/ente.202200892>.

© 2022 The Authors. Energy Technology published by Wiley-VCH GmbH. This is an open access article under the terms of the Creative Commons Attribution-NonCommercial License, which permits use, distribution and reproduction in any medium, provided the original work is properly cited and is not used for commercial purposes.

DOI: 10.1002/ente.202200892



The overall reaction can be performed for hydrogen release at low pressures and reversed at higher pressures for a new storage cycle. The DHC of ethanol distinguishes itself through several beneficial characteristics. First, a mature biogenic carrier is used, which avoids the necessity to utilize fossil resources for manufacturing the storage system carrier. The global production of bioethanol was ≈ 110 billion liters in 2018 and is expected to reach ≈ 140 billion liters per annum by 2022.^[10] Second, the reaction is catalyzed by Cu-based catalysts like copper or copper chromite,^[11] which avoids the noble metal catalysts commonly required for other LOHCs. The reaction is also highly selective for the formation of ethyl acetate in 98–99% over plausible competing aldol and hydrolysis reactions.^[7b] Third, the dehydrogenation reaction is thermodynamically more favorable in the gas phase, which allows hydrogen release under comparatively mild conditions.

In previous work, an analysis of the DHC of ethanol to produce hydrogen and ethyl acetate was performed in the liquid phase using a homogeneous catalyst.^[9] A challenge identified in this study was a poor overall energy efficiency, which arose from the high heating and cooling requirements associated with the reflux of ethanol and ethyl acetate. To address this, the current work presents a thermodynamic analysis of the ethanol–ethyl acetate storage cycle in the gas phase where reflux can be avoided. The study includes both the thermodynamics of the reaction itself, modeling of the technical process, which provides an estimate for the overall efficiency, and a first-order lifecycle assessment of associated greenhouse gas emissions. The study is designed to give a high-level assessment of the viability of the process to determine whether it merits a more in-depth examination of factors including reaction rates, product purity, conversion, and selectivity. The results of this study have relevance for decision-makers in both industry and politics to assist them in identifying reasonable LOHCs that can solve the current challenges in energy storage.

2. Thermodynamics of the Reaction

The thermodynamics for individual reactions, and calculated equilibria under different temperatures and pressures, were calculated using HSC Chemistry 10 (Metso Outotech, Finland). Details and references are provided in the Supporting Information. Formation of ethyl acetate releases 1 mol of H_2 per mole of ethanol (reaction 1). The same stoichiometry of hydrogen release occurs through conversion of ethanol to acetaldehyde in the first reaction step (reaction 2). However, it is advantageous to select reaction conditions that enable further conversion of acetaldehyde and ethanol to form ethyl acetate in a second step (reaction 3). While the first step is clearly endothermic ($\Delta H^{\text{R,gas}} = +63.3 \text{ kJ mol}(\text{H}_2)^{-1}$), the second is exothermic ($\Delta H^{\text{R,gas}} = -40.7 \text{ kJ mol}(\text{H}_2)^{-1}$). Thus, the overall heat demand for hydrogen release can be decreased by about a factor of 6 by forming ethyl acetate ($\Delta H^{\text{R,gas}} = +11.3 \text{ kJ mol}(\text{H}_2)^{-1}$) compared with the sole reaction to acetaldehyde.

Just as important as the reduction in heat demand is the effect on the reaction equilibrium. Due to the pronounced endothermicity, the first reaction step (reaction 2) has a low thermodynamic driving force at low temperatures. The increase in entropy due to the formation of another molecule during dehydrogenation ($\Delta S^{\text{R,gas}} = +114.7 \text{ J mol}^{-1} \text{ K}^{-1}$) is not sufficient to completely compensate the endothermicity, leading to a positive Gibbs free energy of reaction at standard conditions ($\Delta G^{\text{R,gas}} = +29.1 \text{ kJ mol}^{-1}$). On the other hand, the second reaction step (reaction 3), even though accompanied by a slight decrease in entropy ($\Delta S^{\text{R,gas}} = -54.6 \text{ J mol}^{-1} \text{ K}^{-1}$), has a strong thermodynamic driving force at low temperature ($\Delta G^{\text{R,gas}} = -24.5 \text{ kJ mol}^{-1}$). The positive and negative values of the Gibbs energy for the two reaction steps more or less cancel each other ($\Delta G^{\text{R,gas}} = +2.3 \text{ kJ mol}(\text{H}_2)^{-1}$). Therefore, hydrogen release over both reaction steps is thermodynamically feasible under moderate conditions, while hydrogenation for recharging the carrier can still be realized by applying suitable reaction conditions.

As temperature increases, the first reaction step (reaction 2) becomes more favorable, while the second reaction step becomes less favorable. Thus, the concentration of the intermediate acetaldehyde in the reaction mixture can be expected to increase. The overall reaction also becomes more favorable with increasing temperature due to its slight endothermicity. Hence, dehydrogenation is performed best at high temperatures, while hydrogenation should be carried out at low temperatures (and high pressures).

The process model described below employs a pressure of 10 bar for the dehydrogenation reactor. Although lower pressures would favor greater dehydrogenation, pressures significantly above atmospheric simplify mass transport and hydrogen delivery, especially considering that hydrogen comprises only a fraction of the gases exiting the dehydrogenation reactor. In addition, literature reports^[11a] on the synthesis of ethyl acetate from ethanol concluded that pressures of ≈ 10 bar gave the highest space–time yields while also minimizing byproducts derived from acetaldol. Equilibria calculated at this pressure are shown in **Figure 1**. This equilibrium analysis shows that it is not

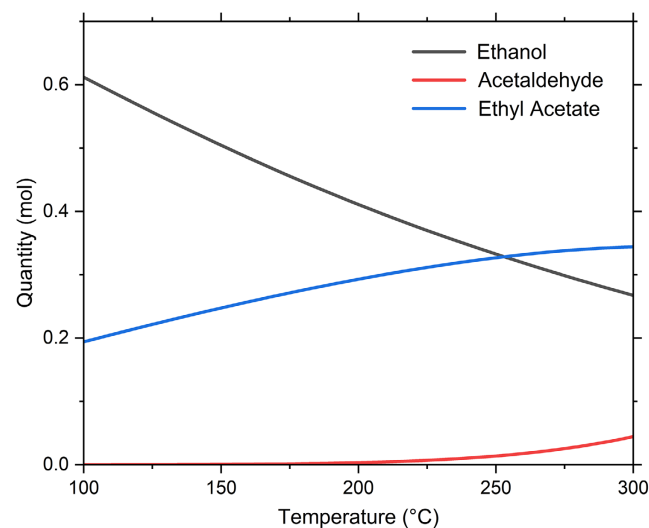


Figure 1. Calculated quantities of organic compounds in equilibrium from 1 mol ethanol at 10 bar total pressure as a function of temperature.

possible to fully dehydrogenate ethanol at 10 bar and at temperatures that are likely to be employed in practice; nevertheless, 68% of ethanol can be converted into products at 260 °C. This temperature was used for the process model where the equilibrium mixture of gases comprises 51% H₂, 25% ethyl acetate, 31% acetaldehyde, and 24% ethanol. The 68% conversion of ethanol leaves a fraction of 24% ethanol (and not 32%) remaining because of the differing numbers of molecules between reactants and products. Acetaldehyde was the only significant byproduct predicted by thermodynamic modeling; the equilibrium concentrations of CO₂, CO, and acetic acid were all negligible.

Equilibrium for the hydrogenation process was modeled at 240 °C. The equilibrium conversion to ethanol increases with increasing pressure (Figure 2a) and the fraction of acetaldehyde

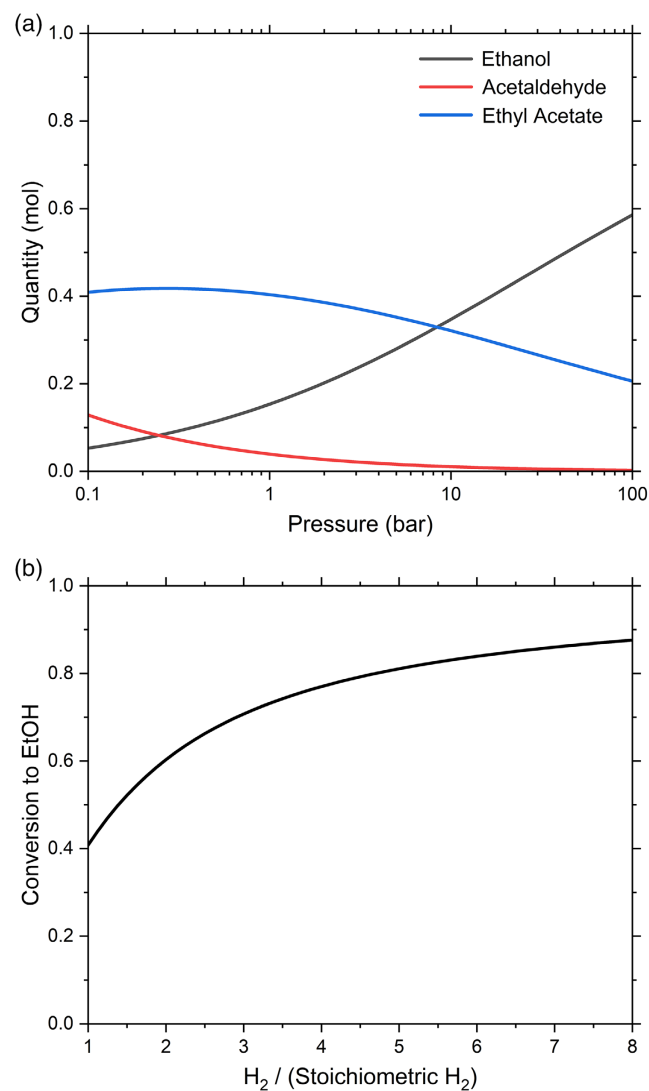


Figure 2. a) Calculated quantities of organic compounds in equilibrium at 240 °C as a function of total pressure, based on 1 mol ethanol if full hydrogenation would be reached. b) Hydrogenation conversion of ethyl acetate to ethanol at 240 °C and 18 bar total pressure with increasing quantities of H₂ input to the calculation. The stoichiometric amount of hydrogen is 1 mol H₂:0.5 mol ethyl acetate.

becomes negligible at pressures larger than 10 bar. This shows that hydrogenation requires high pressure but that the yield of ethanol is still less than 60% even at 100 bar. However, the quantities in Figure 2a are based on a stoichiometric quantity of hydrogen, that is, no H₂ is remaining if ethyl acetate is fully hydrogenated to ethanol. In practice, an excess of H₂ is likely to be applied in the hydrogenation reactor and recycled back to the reactor after separation of the products. Figure 2b shows that this is effective for improving hydrogenation; the equilibrium conversion increases from 41% to 81% at 18 bar, the pressure used in the process modeling, by applying five-times excess of hydrogen.

3. Considerations on Reaction Conditions and Kinetics

There are several results reported in the scientific and patent literature on the gas-phase dehydrogenation of ethanol to ethyl acetate catalyzed by a variety of copper systems, ranging from catalyst development to process design.^[11a,12] These dehydrogenative processes were optimally designed for the production of ethyl acetate with hydrogen as a byproduct, thus providing a different route to ethyl acetate from the conventional esterification of acetic acid with ethanol.^[13] In contrast, the purpose of this study is to maximize the production of hydrogen even at the expense of lower selectivity for ethyl acetate.

The dehydrogenation kinetics used to analyze the process (vide infra) is modeled using a Langmuir–Hinshelwood model and the reaction kinetics and catalyst data obtained from Carotenuto et al.^[14] The cycle starts with the equilibrated adsorption of ethanol followed by dehydrogenation to adsorbed acetaldehyde. The latter reaction is rate determining for the overall dehydrogenation, but does not distinguish between the two elementary hydride transfer steps from the surface intermediates to the metal. The adsorbed acetaldehyde, in equilibrium with gas-phase acetaldehyde, reacts with adsorbed ethanol to produce ethyl acetate in the rate-determining step for reaction 3. A more detailed mechanism proposes the intermediacy of a hemiacetal that dehydrogenates to ethyl acetate.^[11a] Regardless, it is notable and important that Cu catalysts, combined with a reducible oxide (e.g., Cu over ZnO, and copper chromite, Cu₂Cr₂O₅), suppress the dimerization of acetaldehyde to acetaldol.

For the modeling of the hydrogenation reaction, an equilibrium approach was chosen instead of a rate kinetic model. This decision was made based on the assumption that hydrogenation is carried out at a centralized facility, unlike dehydrogenation, which is performed at a site and time of energy demand (like a vehicle or fueling station). Hence, there is no urgent need for high-power density, but rather for high efficiency. Reaching conversions close to the thermodynamic equilibrium seems therefore reasonable for the operation mode of hydrogenation, while dehydrogenation will most likely be limited by reaction kinetics.

4. Process Modeling

This section is intended to show the way the process was modeled to get results regarding energy efficiency in the next section. Further data regarding the model are provided as

supporting information. The block flow diagram of the ethanol–ethyl acetate process is shown in **Figure 3**. A rigorous process model was developed based on literature data, using the Aspen Plus (Version V10) commercial simulation package. Predictive Redlich–Kwong–Soave equation of state is used as the thermodynamic package for modeling purpose. The process is designed to produce 500 kg h⁻¹ of hydrogen.

In this process, ethanol (S1 and S2) is pumped to 10 bar pressure and fed to the dehydrogenation reactor. The fresh ethanol stream (S1) is a make-up for any losses during the cyclic process and is required to maintain the hydrogen production of 500 kg h⁻¹. S2 is the product mixture that is produced in the hydrogenation step (vide infra). The total stream fed to the reactor is heated to 260 °C using the outlet reactor stream (S4) and a furnace. The outlet reactor stream (S4) contains unconverted ethanol, ethyl acetate, acetaldehyde, and hydrogen. Hydrogen must be separated from the other components, and for that purpose, stream S4 is cooled to 40 °C using cooling water (CW), before feeding it to a flash separator vessel. Hydrogen at a purity of 96.3 mol% is recovered in the vapor stream (S5) but needs further purification for application in a fuel cell. To achieve this, stream S5 is compressed to 30 bar and processed through a pressure swing adsorption unit (PSA), to obtain hydrogen at 99.97 mol% purity.^[15] The PSA unit is modeled using a simple separator block with a hydrogen recovery rate of 90%.^[16] The liquid stream (S6) from the flash separator contains a very small fraction (<0.5%) of the hydrogen produced as dissolved H₂ and

passes through a pressure release valve to reduce the pressure to 1 bar. The hydrogen-rich vapor is separated using a second flash vessel, from which the liquid stream (S7), rich in ethyl acetate, is sent to a storage tank.

The hydrogen-rich vapor from the second flash vessel and the impure stream from the PSA unit (labeled “H₂ and other impurities” in Figure 3) are used to offset the dehydrogenation heating requirements. The dehydrogenation reactor is a multitubular plug flow reactor with 50 tubes, *L* = 1.5 m and *D* = 0.65 m. Reactions 2 and 3 are considered in the dehydrogenation reactor.

For hydrogenation, stream (S9) from the LOHC tank is pressurized to 18 bar and mixed with fresh (S10) and recycled hydrogen (S11). It is assumed that the hydrogen from the electrolyzer is available at 20 bar. The molar ratio of H₂ to ethyl acetate + acetaldehyde is 8. This ratio is based on a study by Zhipeng et al.,^[17] in which they used a H₂-to-ethanol molar ratio in the range of 8–16. The reason for a high H₂-to-reactant molar ratio is to avoid catalyst deactivation due to the condensation of the intermediate products, and it also improves the yield as discussed above. The total stream (S9, S10, and S11) is heated to 230 °C using the reactor outlet stream (S13), before feeding it to the hydrogenation reactor. Stream S13 is at a higher temperature than the inlet stream due to the exothermic nature of the reaction, requiring no energy addition once the reaction is initiated. The reactor outlet stream (S13) contains unconverted ethyl acetate and acetaldehyde, ethanol, and hydrogen. It is cooled to 40 °C using cooling water (CW) and fed to a flash separator to separate hydrogen

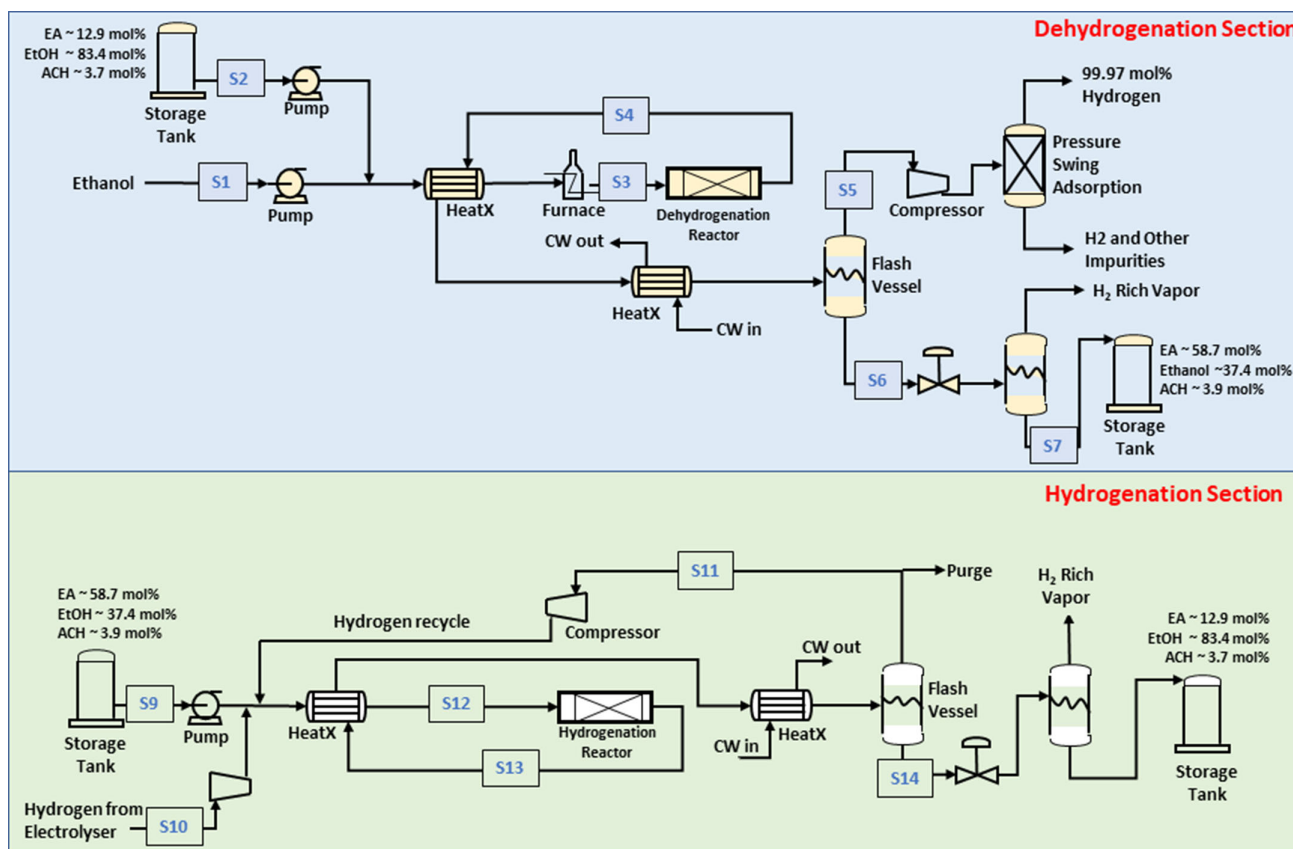


Figure 3. Block flow diagram of ethanol–ethyl acetate LOHC process.

Table 1. Summary of important streams as shown in Figure 1.

	S1	S3	S4	S6	S10	S12	S13	S14
Temperature [°C]	35.0	260	260	40.0	35.0	230	272	40.0
Pressure [bar]	1.013	10	10	9.8	20.0	18.1	18	17.8
Mole flow [kmol h ⁻¹]	18.9	480	617	331	309	2,117	1,988	464
Mass flow [kg h ⁻¹]	871	24 570	24 570	23 305	623	28 375	28 375	23 752
Mole fraction								
Ethanol	1.00	0.840	0.205	0.373		0.0652	0.201	0.830
Acetaldehyde		0.0354	0.0245	0.0392		9.54E-03	0.0125	0.0371
Ethyl acetate		0.124	0.322	0.585		0.0943	0.0334	0.1288
Hydrogen		1.79E-04	0.448	3.27E-03	1.00	0.831	0.753	4.58E-03

from the remaining components. Stream S11 containing 98.1 mol% pure hydrogen is recycled to the hydrogen reactor. The model purge of 3% for stream S11 is to avoid build-up of hydrogen in the system for the purpose of the model, although the purge may not be required in practice. The liquid stream S14 containing 83 mol% pure ethanol is passed through a pressure release valve to reduce the stream pressure to 1 bar. About 0.63% of the stream (S14) is vaporized which is separated using a flash vessel, and the liquid is stored in a tank for future use. A summary of important streams is shown in **Table 1**.

It should be noted that the heat exchanger network is designed using the Aspen Energy Analyzer and scientific judgment. Recuperators are used for both the hydrogenation and dehydrogenation processes to recover the sensible and latent heat from the reactor exits and use it to preheat the reactor feed streams. A minimum temperature approach of 10 °C was used to size these heat exchangers and significantly improve the overall process efficiency.

5. Energy Efficiency and Environmental Impact

The energy input and output for the overall process is shown in **Table 2**. The lower heating value (LHV) was used to quantify the energy input for hydrogen and purge streams. An efficiency of 80% was assumed for the recovery of heat available from the purge streams. Electricity usage includes the power required for pumping the feed streams, for H₂ compressors, and to circulate the cooling water through the heat exchangers.

It was assumed that a natural gas (NG)-fired furnace will be utilized to keep the endothermic dehydrogenation reactor at a desired temperature and for heating the feed streams. For dehydrogenation, the purge stream in **Table 2** is the sum of the impurities separated by the compressor and PSA units, and the vapor separated in the second, low-pressure, flash vessel. For hydrogenation, the purge stream is the sum of the purge from S11 and the H₂-rich vapor from the low-pressure flash vessel. All these individual streams contain H₂, ethanol, ethyl acetate, and acetaldehyde in various proportions. The Aspen models required this quantity of purge to reach convergence, although a smaller purge might be achievable in practice.

The overall process efficiency is estimated to be 88%, calculated using Equation (4). In the efficiency (*Eff*) calculation, the available hydrogen energy recovered from dehydrogenation is divided by the energy demand of hydrogenation.

Table 2. Summary of process energetics.

Energy input	kW
Electricity (Elec)	433
Pumps and compressors	378
Cooling water circulation	55
Make-up ethanol	6460
Natural gas (NG)	3,442
Dehydrogenation feed heat	2,126
Dehydrogenation reactor	1,316
Hydrogen (H ₂ , LHV)	20 903
Energy output	
	kW
Hydrogen (99.97 mol%, LHV)	16 691
Purge streams (PS, LHV)	15 427
Dehydrogenation section	11 070
Hydrogenation section	4,357
Energy efficiency	88%

$$Eff = \frac{\text{Available Dehydrogenation Energy}}{\text{Hydrogenation Energy Demand}} \quad (4)$$

The energy balances of hydrogenation and dehydrogenation are defined by Equation (5) and (6).

$$\begin{aligned} &\text{Available Dehydrogenation Energy} \\ &= H_2 \text{ Released} - (\text{Heat Required} - \text{Recoverable Waste Heat}) \end{aligned} \quad (5)$$

$$\begin{aligned} &\text{Hydrogenation Energy Demand} \\ &= H_2 \text{ Provided} - \text{Purged } H_2 \text{ Credit} \\ &\quad + \text{Electricity Required} \end{aligned} \quad (6)$$

The hydrogen provided and released, recoverable waste heat from the respective purge streams, NG heating required, and energy input for pumps and compressors used in this calculation are provided in **Table 2**.

The electricity usage by pumps, compressors, and cooling water circulation is shown in **Figure 4**. Heat, provided by NG combustion, is the main form of energy demand. However,

the higher exergetic value of electric energy should be kept in mind. The majority of the electricity is used in compressing the hydrogen for purification by the PSA unit. This shows that electric energy demand during dehydrogenation depends on purity requirements. If lower hydrogen purity is acceptable, this energy demand could be avoided to some extent. Among the two process sections, the dehydrogenation section constitutes $\approx 80\%$ of the total electricity usage in the process. This is particularly relevant as dehydrogenation is performed at sites or times of energy demand, while hydrogenation can be done at sites or times of excess energy. The electric energy demand could be reduced significantly if a lower hydrogen purity is acceptable. The NG requirement is high in the dehydrogenation section due to the heat demand of the reaction. Approximately 60% of the NG is required for keeping the dehydrogenation reactor at setpoint. This is a comparatively low proportion compared to other hydrogen carriers like H0-/H18-DBT and can be explained by the lower endothermicity and reaction temperature.

The derived values for energy demand have been utilized to perform an assessment of the ecobalance. Lifecycle greenhouse gas emissions associated with storing and delivering 1 kg of hydrogen in a large-scale system were estimated. The system was assumed to supply 500 kg h^{-1} hydrogen to a fuel cell backup power system for 172 h per year for 20 years in the United States. The hypothetical system would require 12.8 ton of dry-mill corn ethanol as an initial fill in year one and 62.7 ton of ethanol makeup per year. All upstream and direct emissions associated with the production of NG,^[18] electricity,^[19] and ethanol^[20] (51.4 kg $\text{CO}_{2\text{eq}}$ kJ^{-1} ethanol) were included using average or central best estimate emission factors for the USA. Emissions from the ethanol itself were assumed to be biogenic carbon dioxide and therefore do not contribute to lifecycle greenhouse gas emissions.

The ethanol storage system would have a carbon intensity of 7.0 kg- $\text{CO}_{2\text{eq}}$ kg-H_2^{-1} delivered, 36% of which is associated with the first fill (Table 3). The carbon intensity would decrease to 6.6 kg- $\text{CO}_{2\text{eq}}$ kg-H_2^{-1} in the event that wind electricity^[21] is used.

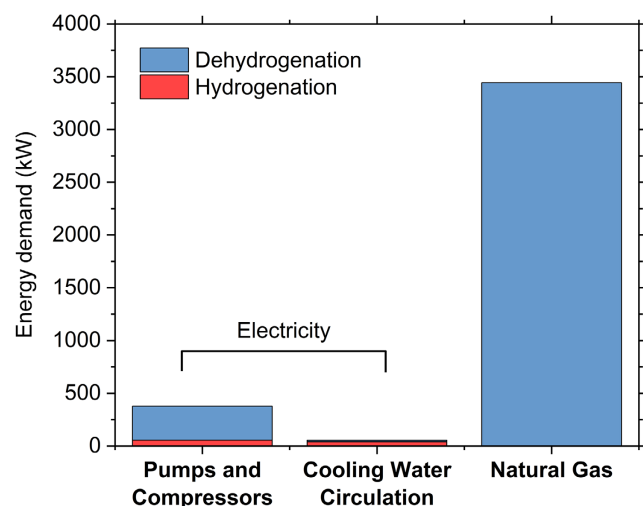


Figure 4. Breakdown of energy usage in the dehydrogenation and hydrogenation section (hydrogen release rate corresponding to about 500 kg h^{-1} and corresponding to a 16 691 kW expressed in terms of LHV).

Table 3. Greenhouse gas emissions for a storage system operating 172 h year^{-1} at 500 kg- H_2 h^{-1} , normalized over a 20-year lifespan. Upstream emissions associated with energy consumption are based on current US averages.

Source	Normalized greenhouse gas emissions kg- $\text{CO}_{2\text{eq}}$ kg-H_2^{-1}
Initial fill ethanol	2.49
Pumps and compressors	0.34
Cooling water recirculation	0.05
Dehydrogenation feed heat	0.22
Dehydrogenation reactor	0.14
Direct NG emissions	1.28
Make-up ethanol	2.45
TOTAL	6.97

If no ethanol makeup was needed, the carbon intensity would decrease to 4.5 kg- $\text{CO}_{2\text{eq}}$ kg-H_2^{-1} . More likely, the ethanol and hydrogen in the system's purge streams could be used to offset NG consumption for the dehydrogenation reactor and feed heat, and in this case the carbon intensity would drop to 5.3 kg- $\text{CO}_{2\text{eq}}$ kg-H_2^{-1} . If wind electricity and ethanol with just half the carbon intensity of dry-milled corn ethanol were used along with purge gas combustion, the storage system's carbon intensity would decrease to 2.7 kg- $\text{CO}_{2\text{eq}}$ kg-H_2^{-1} . This shows that conclusions on the ecological impact should be done with caution as there is a significant sensitivity on different parameters. A comparison to noncarrier based storage is likely show a slightly higher impact as the provision of the carrier requires some effort, which causes ecological impact. As a comparison, the carbon intensity of 350 bar compressed gas and cryogenic hydrogen (liquid hydrogen) storage for hydrogen truck transportation applications assuming average grid electricity has been reported as 2 and 5.2-8 kg- $\text{CO}_{2\text{eq}}$ kg-H_2^{-1} ,^[22] respectively. This suggests that low-carbon ethanol may have an advantage over liquid storage from a carbon emissions perspective. Comparing the approach to fossil carriers a clear advantage can be expected.

6. Comparison to Other Carriers

The ethanol-ethyl acetate system can be operated at a higher efficiency than is reached by most alternative hydrogen carriers. LOHCs based on reversible hydrogenation of aromatic double bonds (as in the case of the H0-/H18-DBT system) usually require about 30% of the energy content of the hydrogen for release.^[23] A recent techno-economic analysis^[24] of several LOHCs found storage efficiencies of 60.8% for H18-DBT and 53.8% for methylcyclohexane when the heat released during hydrogenation was not recovered. By comparison, the analysis in this work indicates 88% energy efficiency for the much cheaper ethanol-ethyl acetate storage cycle.

Although more energy efficient, ethanol has a lower energy storage density compared to hydrocarbons. The gravimetric hydrogen storage capacity of ethanol is only 4.3 mass% (compared to 6.2 mass% for H18-DBT) and the volumetric capacity 35 g(H_2) L^{-1} (57 g(H_2) L^{-1} for H18-DBT). Thus, the

ethanol-based system still seems suited for applications requiring high energy density. Yet, in high-energy-content applications, other carriers could be superior.

An interesting aspect of the ethanol–ethyl acetate system is the fact that it is a biogenic hydrogen carrier material. While most other LOHCs are derived from fossil resources (often via toluene), ethanol is derived by a fermentation of biomass. If ethanol can be produced with a carbon intensity lower than corn ethanol, a sustainable, large-scale provision of the carrier is possible, which is challenging for most other organic carriers. Considering that ethanol may be recycled in this process many times or used to replace NG, the system could have a carbon intensity lower than cryogenic hydrogen storage.

7. Conclusion

The reversible dehydrogenation of gaseous ethanol to ethyl acetate has been evaluated thermodynamically to understand the equilibrium and efficiency of the process. The equilibrium shifts considerably between hydrogenation and dehydrogenation at temperatures between 200 and 300 °C and pressure less than 100 bar. Although conversions of 100% of either hydrogenation or dehydrogenation are not feasible, the range can be maximized using a low dehydrogenation temperature and an excess of hydrogen for hydrogenation. The thermodynamic boundary conditions enable a reasonable storage cycle without applying extreme reaction conditions.

Process modeling of the overall cycle shows that an energy efficiency of 88% can be achieved. This is a comparatively high value compared to other hydrogen carriers and can be attributed mainly to the very low endothermicity of the hydrogen release reaction. Further improvements of efficiency might, for instance, be realized through integration of external waste heat sources for dehydrogenation. Because the reaction can be performed at lower temperatures than for other hydrogen carriers, such thermal integration could be simplified. The calculated greenhouse gas emissions are dominated by contributions from the ethanol used in the first fill and added during each cycle to make up for material losses. The ethanol/ethyl acetate system is not only interesting because of the utilization of a biogenic carrier, but also due to a prospective high efficiency. The results of this study suggest that the system warrants a more detailed examination of factors such as: the kinetics as a function of feedstock composition, whether conversion and selectivity are consistent over a number of complete cycles, and whether minor side products build up and degrade performance.

Supporting Information

Supporting Information is available from the Wiley Online Library or from the author.

Acknowledgements

This work was supported by the US Department of Energy (DOE), Office of Energy Efficiency and Renewable Energy. The authors gratefully acknowledge research support from the Hydrogen Materials - Advanced Research Consortium (HyMARC), established as part of the Energy Materials

Network under the U.S. Department of Energy, Office of Energy Efficiency and Renewable Energy, Hydrogen and Fuel Cell Technologies Office, under contract number no. DE-AC36-08GO28308. Pacific Northwest National Laboratory was operated by Battelle for the U.S. Department of Energy.

Open Access funding enabled and organized by Projekt DEAL.

Conflict of Interest

The authors declare no conflict of interest.

Data Availability Statement

The data that support the findings of this study are available from the corresponding author upon reasonable request.

Keywords

bioresources, hydrogen storage, organic carriers, process models

Received: August 5, 2022

Revised: September 21, 2022

Published online: October 27, 2022

- [1] a) T. He, P. Pachfule, H. Wu, Q. Xu, P. Chen, *Nat. Rev. Mater.* **2016**, *1*, 16059; b) K. Müller, M. Felderhoff, *Energy Technol.* **2018**, *6*, 443; c) M. R. Usman, *Renewable Sustainable Energy Rev.* **2022**, *167*, 112743; d) M. Wieliczko, N. Stetson, *MRS Energy Sustainability* **2020**, *7*, E41.
- [2] a) M. Amende, S. Schernich, M. Sobota, I. Nikiforidis, W. Hieringer, D. Assenbaum, C. Gleichweit, H.-J. Drescher, C. Papp, H.-P. Steinrück, A. Görling, P. Wasserscheid, M. Laurin, J. Libuda, *Chem. Eur. J.* **2013**, *19*, 10854; b) P. T. Aakko-Saksa, C. Cook, J. Kiviaho, T. Repo, *J. Power Sources* **2018**, *396*, 803; c) P. M. Modisha, C. N. M. Ouma, R. Garidzirai, P. Wasserscheid, D. Bessarabov, *Energy Fuels* **2019**, *33*, 2778.
- [3] K. Müller, J. Völkl, W. Arlt, *Energy Technol.* **2013**, *1*, 20.
- [4] M. Taube, D. Rippin, W. Knecht, D. Hakimifard, B. Milisavljevic, N. Gruenfelder, *Int. J. Hydrogen Energy* **1985**, *10*, 595.
- [5] N. Brückner, K. Obesser, A. Bösmann, D. Teichmann, W. Arlt, J. Dungs, P. Wasserscheid, *ChemSusChem* **2014**, *7*, 229.
- [6] a) C. A. Chagas, R. L. Manfro, F. S. Toniolo, *Catal. Lett.* **2020**, *150*, 3424; b) M. Taghizadeh, F. Aghili, *Rev. Chem. Eng.* **2019**, *35*, 377.
- [7] a) O. A. Ferretti, J. P. Bournonville, G. Mabilon, G. Martino, J. P. Candy, J. M. Basset, *J. Mol. Catal.* **1991**, *67*, 283; b) E. Santacesaria, G. Carotenuto, R. Tesser, M. Di Serio, *Chem. Eng. J.* **2012**, *179*, 209.
- [8] V. Yadav, G. Sivakumar, V. Gupta, E. Balaraman, *ACS Catal.* **2021**, *11*, 14712.
- [9] B. L. Tran, S. I. Johnson, K. P. Brooks, S. T. Autrey, *ACS Sustainable Chem. Eng.* **2021**, *9*, 7130.
- [10] B. Sharma, C. Larroche, C.-G. Dussap, *Bioresour. Technol.* **2020**, *313*, 123630.
- [11] a) K. Inui, T. Kurabayashi, S. Sato, *J. Catal.* **2002**, *212*, 207; b) A. B. Gaspar, F. G. Barbosa, S. Letichevsky, L. G. Appel, *Appl. Catal. A: General* **2010**, *380*, 113.
- [12] a) W. A. Lazier, E.I. Du Pont de Nemours and Co., **1934**; b) K. Turner, M. Sharif, J. Scarlett, A. B. Carter, G. Webb, Davy McKee (London) Limited, **1991**.

- [13] S. W. Colley, C. R. Fawcett, C. Rathmell, M. W. M. Tuck, Johnson Mathey Davey Technologies Ltd., **2004**.
- [14] G. Carotenuto, R. Tesser, M. Di Serio, E. Santacesaria, *Catal. Today* **2013**, 203, 202.
- [15] a) Z. Du, C. Liu, J. Zhai, X. Guo, Y. Xiong, W. Su, G. He, *Catalysts* **2021**, 11, 393; b) J. M. Ohi, N. Vanderborgh, S. Ahmed, R. Kumar, D. Papadius, T. Rockward, Office of Energy Efficiency and Renewable Energy, Washington, DC **2016**.
- [16] C. Allevi, G. Collodi, in *Integrated Gasification Combined Cycle (IGCC) Technologies* (Eds: T. Wang, G. Stiegel), Woodhead Publishing, Sawston **2017**, pp. 419–443.
- [17] Z. Lu, H. Yin, A. Wang, J. Hu, W. Xue, H. Yin, S. Liu, *J. Ind. Eng. Chem.* **2016**, 37, 208.
- [18] a) T. J. Skone, J. Littlefield, J. Marriott, G. Cooney, M. Jamieson, J. Hakian, G. Schivley, *Life Cycle Analysis of Natural Gas Extraction and Power Generation*, No. DOE/NETL-2015/1714, National Energy Technology Laboratory (NETL), Pittsburgh, PA, Morgantown, WV, United States **2016**, <https://doi.org/10.2172/1480993>; b) AP 42, *External Combustion Sources*, fifth ed., Vol. 1 **2016**, Chapter 1, <https://www3.epa.gov/ttn/chieff/ap42/ch01/> (accessed: April 2022).
- [19] L. Chen, A. P. Wemhoff, *Appl. Energy* **2021**, 292, 116898.
- [20] M. J. Scully, G. A. Norris, T. M. Alarcon Falconi, D. L. MacIntosh, *Environ. Res. Lett.* **2021**, 16, 043001.
- [21] S. L. Dolan, G. A. Heath, *J. Ind. Ecol.* **2012**, 16, 136.
- [22] M. Wang, *The Greenhouse Gases, Regulated Emissions, and Energy Use in Transportation (GREET) Model Version 1.5*, <https://www.who.int/news-room/fact-sheets/detail/cardiovascular-diseases-cvds> (accessed: April 2022).
- [23] a) K. Müller, *ChemBioEng Rev.* **2019**, 6, 72; b) K. Müller, *ChemBioEng Rev.* **2019**, 6, 81.
- [24] M. Niermann, S. Drünert, M. Kaltschmitt, K. Bonhoff, *Energy Environ. Sci.* **2019**, 12, 290.